A Novel Small Molecule Inhibitor of CBL-B Shows Potent Antitumor Activity in Combination with Pmel-1 Adoptive Cell Transfer in an Aggressive Mouse Melanoma Model

Marilena Gallotta, Jose Gomez Romo, Serena Ranucci, Austin Tenn-McClellan, Frederick Cohen, Gwenn M Hansen, Arthur T Sands, Ryan Rountree, Cristiana Guiducci

Nurix Therapeutics, San Francisco, CA, USA

Introduction

CBL-B: A Modulator of T Cell Activation and a Novel Target for Immuno-oncology

- CBL-B is an E3 ubiquitin ligase that is expressed in and regulates immune cells, including T, B, NK and dendritic cells
- Mice deficient in CBL-B demonstrate enhanced signal-dependent T cell activation and robust T and NK cell dependent anti-tumor activity
- In T cells, CBL-B limits cell activation following TCR engagement, enforcing the need of CD28 co-stimulation
- Inhibition or deletion of CBL-B increases IL-2 production in T cells upon stimulation and enhances the immune response
- Inhibiting CBL-B with a small molecule represents a novel immunotherapy target opportunity to overcome checkpoint resistance and reduce effects of the suppressive tumor microenvironment
- CBL-B inhibition during *in vitro* activation of tumor-specific T cells profoundly improves their functionality and ability to control tumor growth following ACT in tumor-bearing mice
- Here we utilize NX-0255-treated Pmel-1 ACT/B16 melanoma tumor model to compare the antitumor effect of post infusion *in vivo* treatment with NX-1607 to high dose IL-2

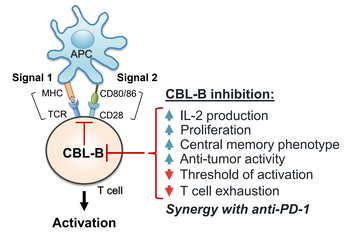

NX-1607: Optimized CBL-B inhibitor for oral delivery. NX-1607 is currently in a Phase 1a clinical trial in patients with advanced solid tumors NX-1607-101 (NCT05107674).

NX-0255: Optimized CBL-B inhibitor for *ex vivo* use. Developing in conjunction with autologous TIL cell therapies as DeTIL-0255 in a Phase 1a clinical trial for gynecologic malignancies (NCT05107739)

Background

Figure 1. ACT with NX-0255-treated Pmel-1 is Associated with Increased Antitumor Activity, Persistence and Memory Phenotype

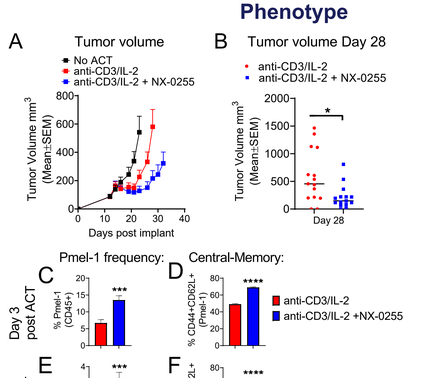

(A-B) Mice bearing B16-OVA s.c. tumors were treated IV on Day 13 with ACT of CD3-stimulated Pmel-1 T cells that were cultured in the presence of either 300 IU/mL IL-2 or 1 µM NX-0255 and 300 IU/mL IL-2. No ACT control mice were administered only media IV. (B) Statistical significance of differences in mean tumor volumes between groups on Day 28 was evaluated using Mann-Whitney U test (P > 0.05, * P ≤ 0.05, ** P ≤ 0.01, *** P ≤ 0.001, and **** P ≤ 0.0001). (C-F) On Day 16 (3 days after ACT) and Day 26 (13 days after ACT) blood was collected from all ACT-treated animals and frequency of Pmel-1 cells (% of CD45+ cells) and frequency of Pmel-1 cells with central-memory phenotype was determined by flow cytometry (C and D, Day 3 post ACT; E and F, Day 13 post ACT). Mann-Whitney U test (*** P ≤ 0.001, and **** P ≤ 0.0001).

Results

Figure 2. ACT Supported by *in vivo* Treatment with NX-1607 Increases the Antitumor Activity of NX-0255-treated Pmel-1 Cells

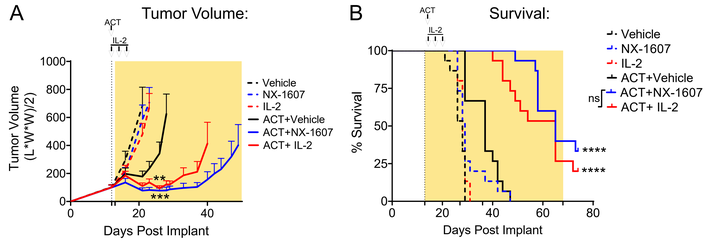

(A-B) Mice bearing B16-OVA s.c. tumors were treated IV on Day 13 with ACT of CD3-stimulated Pmel-1 T cells that were cultured in the presence of 300 IU/mL IL-2 plus 1 µM NX-0255 (continuous lines). No ACT control mice were administered only media IV (dotted lines). Mice were then treated with either NX-1607, 30 mg/kg, po QD for 8 weeks (shaded area), or 150,000 IU IL-2, i.p. BID for 3 consecutive days. In both graphs (A, tumor volume, and B, survival), dotted lines represent *in vivo* treatment controls with no ACT. (A) Statistical significance of differences in mean tumor volumes between groups on Day 28 was evaluated using Mann-Whitney U test (** P ≤ 0.01 and *** P ≤ 0.001). (B) Statistical significance of differences in survival between groups was evaluated using the Log-rank (Mantel-Cox) test (ns P > 0.05, and **** P ≤ 0.0001).

Figure 3. NX-1607 in Combination with ACT Enhances the Quality of Transferred NX-0255-treated Pmel-1 in Circulating Cells, Inducing a More Memory-like and Cytotoxic Phenotype Compared to IL-2

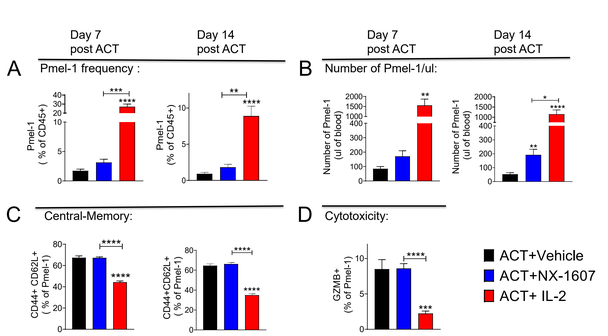

(A-D) Blood was collected from all ACT-treated animals (see Figure 2) on Day 20 (7 days after ACT) and Day 27 (14 days after ACT) and frequency of Pmel-1 cells (% of CD45+ cells, A), total number of Pmel-1 cells in the blood (per mL of blood, B), frequency of Pmel-1 cells with central-memory (C) and cytotoxic (D) phenotype was determined by flow cytometry. Group mean values ± SEM are shown in each graph. Statistical significance was determined Kruskal-Wallis test (*** P ≤ 0.001, and **** P ≤ 0.0001).

Figure 4. NX-1607 in Combination with ACT Enhances the Quality of Transferred NX-0255-treated Pmel-1 in the Tumor, Inducing a More Stem Cell-like Memory Phenotype Compared to IL-2

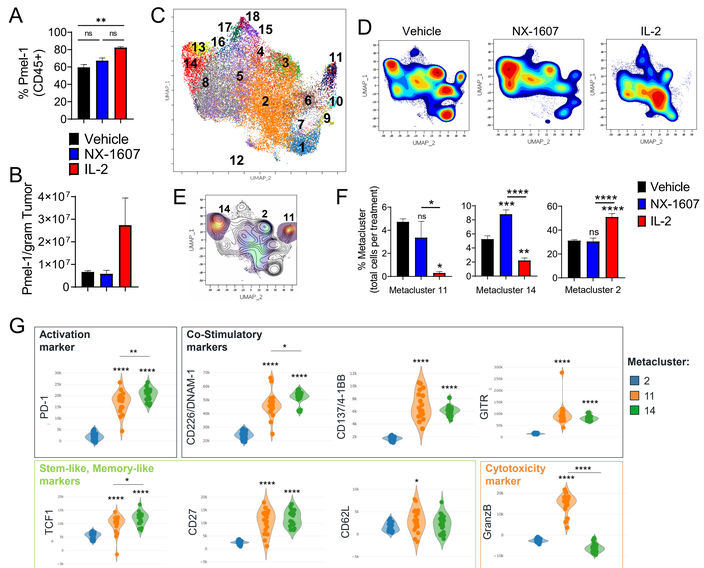

- ACT + NX-1607 compared to ACT + IL-2 treatment resulted in accumulation of intratumoral Pmel-1 T cells characterized by expression of stem cell-like memory markers (Metacluster 14) and stem cell-like memory markers with the cytotoxic marker GranzB (Metacluster 11).
- ACT + IL-2 treatment resulted in higher representation of Pmel-1 T cells characterized by a generally less activated phenotype (Metacluster 2).

(A-G) B16-OVA tumors from mice treated by administration of either: vehicle control (po, QD) or NX-1607 at 30 mg/kg (po, QD) or IL-2 at 150,000 IU (ip, BID for 3 days) were collected from all ACT-treated animals (see Figure 2) on Day 20 (7 days after ACT) and investigated for T cell phenotypic change by Flow Cytometry and Dimensionality Reduction analysis. (A-B) Frequency of Pmel-1 cells (% of CD45+ cells, A) and total number of Pmel-1 cells (per gram of tumor, B) were determined by flow cytometry. Group mean values ± SEM are shown in each graph. Statistical significance was determined by Kruskal-Wallis test (** P ≤ 0.01). (C) UMAP plots of Pmel-1 cells overlaid with color-coded T cell clusters identified by FlowSOM. (D) Density UMAP plots of Pmel-1 cells from each treatment group. The clusters with statistically significant differences between treatment groups are highlighted on UMAP plot (E) with corresponding cell frequency bar graph (means ± SEM) (F). (G) Violin plots displaying the expression level of selected markers on identified Pmel-1 cell clusters. Statistical significance using Kruskal-Wallis test: * P ≤ 0.05, ** P ≤ 0.01, *** P ≤ 0.001, and **** P ≤ 0.0001.

Conclusions

- **Treatment of CD3-stimulated tumor-specific Pmel-1 cells using NX-0255, a novel small molecule CBL-B inhibitor, is associated with increased anti-tumor activity, increased persistence and memory phenotype in tumor and blood following adoptive transfer in an aggressive mouse melanoma model.**
- **NX-1607 in combination with ACT enhances the quality of transferred NX-0255-treated Pmel-1 in circulating cells and in tumor, inducing a more memory-like and cytotoxic phenotype compared to IL-2.**
- **The observed antitumor effects of NX-1607 support its potential use in combination with cell-based therapeutics.**
- **Nurix is using NX-0255 in the production of an investigational drug-enhanced TIL therapy, DeTIL-0255, which is currently in a Phase 1 clinical trial [NCT05107739].**

Other NX-1607 posters presented at SITC 2022

#777 (Nov. 10th) Whelan S, et al. *Initial clinical characterization of novel proximal biomarkers for NX-1607, a first-in-class oral CBL-B inhibitor, in patients with advanced malignancies.*

#824 (Nov. 11th) Gallotta M, et al. *NX-1607, a small molecule inhibitor of the CBL-B E3 ubiquitin ligase, promotes T and NK cell activation and enhances NK-mediated ADCC in a mouse lymphoma tumor model.*

Other DeTIL-0255 posters presented at SITC 2022

#671 (Nov. 10th) Girda E, et al. *Trial in Progress: A phase 1 adoptive cell therapy using drug-enhanced, tumor-infiltrating lymphocytes, DeTIL-0255, in adults with advanced malignancies.*

#361 (Nov. 10th) Murthy P, et al. *Universal expansion of CBL-B-inhibited tumor infiltrating lymphocytes, DeTIL-0255, from women with ovarian cancer: process validation.*

#254 (Nov. 11th) Liang X, et al. *The CBL-B inhibitor, NX-0255, enhances human drug enhanced tumor infiltrating lymphocyte (DeTIL) expansion and T cell function in full-scale runs.*

Presented at the 37th SITC Annual Meeting, Nov. 8–12, 2022